Adsorption properties of cryptand 222 at the charged mercury-solution interface

Adsorption Properties of Cryptand 222 at the Charged Mercury–Solution Interface

Marcello Carlà and Cecilia M. C. Gambi

Dipartimento di Fisica, Università di Firenze,
Largo E. Fermi 2, I50125 Firenze, Italy

Piero Baglioni

Dipartimento di Chimica, Università di Firenze,
Via G. Capponi 9, I50121 Firenze, Italy

The Journal of
Physical Chemistry®

Reprinted from
Volume 100, Number 26, Pages 11067–11071

Adsorption Properties of Cryptand 222 at the Charged Mercury−Solution Interface

Marcello Carlà* and Cecilia M. C. Gambi

Dipartimento di Fisica, Università di Firenze, Largo E. Fermi 2, I50125 Firenze, Italy

Piero Baglioni

Dipartimento di Chimica, Università di Firenze, Via G. Capponi 9, I50121 Firenze, Italy

Received: January 2, 1996; In Final Form: April 10, 1996[⊗]

The adsorption of the macrocyclic ligand kryptofix 222 at the mercury−water interface has been studied as a function of the polarization potential and the ligand concentration. An automated apparatus has been used to measure interfacial tension by the drop−shape technique. The relative surface excess and the surface charge density have been obtained, and from these parameters, the molecular packing at the interface and the free energy of adsorption have been calculated. The results show that the macrocyclic ligand strongly adsorbs at the interface in the presence of an intermolecular repulsive electrostatic contribution due to Na^+ cations trapped inside the macrocyclic cage. Moreover the adsorption driving force is similar to that reported for the adsorption of aliphatic compounds, i.e., the hydrophobic repulsion of the exposed molecular surfaces.

Introduction

Macrocyclic compounds have been studied in considerable depth due to the large number of applications. Typical examples are separation of ions and isotopes, transport across oil−water interfaces, liquid−liquid and liquid−solid phase transfer reactions, dissolution of organic salts in apolar solvent, ion-selective electrodes, etc.[1−4] A major thrust of many of these studies has been the investigation of the properties associated with cyclic ligand complexes or more sophisticated ligands such as calixarenes, cyclophanes, and other hosts.[5−7] In particular, investigation of spectral, structural, thermodynamical, and electrochemical aspects of macrocyclic−ion complex formation have all received considerable attention.[8−9]

In spite of this large number of studies, poor attention has been devoted to the investigation of the surface properties of macrocyclic compounds. This point is very important since the properties of these compounds can be altered by the "molecular ordering" imposed by the interface of organized structures such as micelles, microemulsions, lamellar phases, or simply the solid−liquid and liquid−liquid interfaces. Furthermore these studies are important for the understanding and mimicking of more complex functions such as photochemical charge separation in organized redox chains, catalysis in enzyme−coenzyme substrate complexes, molecular aggregates with specific functions, etc. For example, Graëtzel et al.[10] showed that micelles of [tetraaza-12-crown-4]−$C_{14}H_{29}$ can be used to store electrons in the presence of Cu^{2+}; Baglioni et al.[11−14] showed that the quantum yield of the photoionization of *N,N,N′,N′*-tetramethylbenzidine is increased in micelles upon complexation of micellar counterions by 15-crown-5 and 18-crown-6. Many other applications have been reported.[15−17]

It was recently shown that macrocyclic ligands can alter the aggregational behaviors of micelles by interaction with the hydrophilic outer layers of the micelles. Three ligands differing by the counterion complexation ability and by the size and shape, i.e., crown ethers, kryptands, and a small macrobicyclic cage, have been used, and the results indicate that macrocycles interact with micelles by adhering to the hydrophilic layers of the micelles and changing the micellar charge size and shape.[18−22] In particular the screening of the micellar charge is strongly affected by the nature of the macrocyclic ligand, suggesting that the size and the orientation of the ligands at the micellar surface play an important role in the counterions complexation.

In this study we report the adsorption properties of the ligand 4,7,13,16,21,24-hexaoxa-1,10-diazabicyclo[8.8.8]hexacosan (kryptofix 222) onto mercury drop electrode as a function of the polarization potential, φ, of the electrode and the ligand concentration, c. By this way we were able to measure the relative surface excess, Γ, the surface charge density, σ_M, and, from these parameters, the packing and the free energy of adsorption of Kryptofix 222 (K222). The results show the presence of an intermolecular repulsive electrostatic term contributing to the free energy of adsorption. This last indicates that the complexed charge is not fully screened upon ligand complexation, suggesting an explanation for the different behavior of macrocyclic ligands in micellar solutions.

Experimental Section

Adsorption properties of K222 have been determined by measuring interfacial tension γ at the mercury−electrolytic solution interface over the concentration range $c = (0.3 \times 10^{-6})-(1 \times 10^{-2})$ M and the polarization potential range $\varphi =$ 0 to −1600 mV (measured with respect to an Ag/AgCl reference electrode). Measurements have been performed using the drop−shape technique with a sessile drop of about 6 mm diameter. The experimental apparatus, controlled by a microVAX computer, has been described elsewhere.[23]

Reagents were Kryptofix 222 (purity > 99%) and NaCl, both from Merck, Suprapur grade; mercury was purified by repeatedly washing in concentrated NaOH and HNO_3 alternatively; water was obtained by a Millipore Milli-Q purifying system fed with spring water with low mineral content. Kryptofix 222 and NaCl were used without any further purification. Disaeration was accomplished by wet nitrogen (from Rivoira, Chivasso, Italy) with purity grade 5.5. The residual oxygen level in the measuring cell was monitored by passing the gas flow from the cell outlet to an O_2-selective electrode (from ECD, Florence, Italy). An O_2 level less than 20 ppm was ascertained during all measurements.

[⊗] Abstract published in *Advance ACS Abstracts,* May 15, 1996.

S0022-3654(96)00031-7 CCC: $12.00

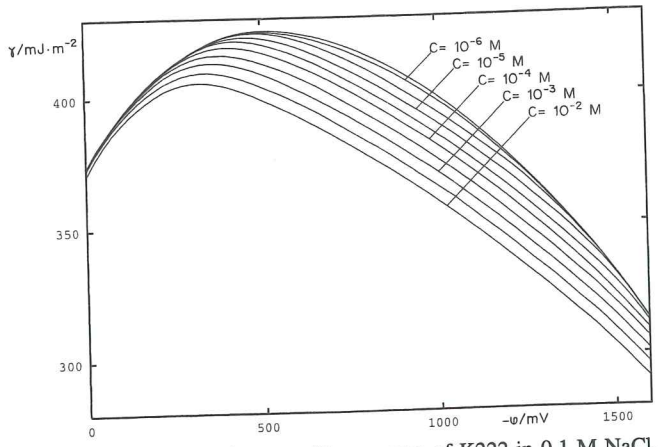

Figure 1. Family of electrocapillary curves of K222 in 0.1 M NaCl. Only two curves per decade are shown.

The concentration range has been scanned in logarithmic steps with eight steps per decade. Each concentration value was obtained by mixing into the measuring cell proper amounts of 0.1 M NaCl solution and one of the following stock solutions: (a) 0.1 M NaCl + 10 mM K222 (measurements in the range from 31.6 μM to 10 mM), (b) 0.1 M NaCl + 100 μM K222 (from 0.316 μM to 100 μM), and (c) 0.1 M NaCl + 10 μM K222 (from 0.316 to 10 μM).

For each concentration value a full electrocapillary curve was taken five times on five mercury drops of about 60 μL. The potential range was scanned in 25 mV steps, and five drop images were taken for every potential value. The solution as well as the drop volumes were dispensed by three automatic dispenser Dosimat 665 instruments Metrohm, Herisau, CH).

At concentrations above 10^{-4} M, a time delay of about 2.5 s was enough after each potential variation to reach adsorption/desorption equilibrium; in the range 10^{-5}–10^{-4} M, the time delay was increased to 20 s. For concentrations below 10^{-5} M, the time delay was further increased to 40 s. However, in this last concentration range the equilibrium was scarcely attained, as proved by a comparison between curves obtained with opposite potential scan direction in a given solution: In the potential regions where adsorption is changing most rapidly, the curve for which desorption is occurring always lies below the one in which adsorption is increasing. As these hysteresis loops are small as compared to the overall effect, the equilibrium values have been extrapolated by averaging the values obtained with forward and backward potential scanning.

Results and Discussion

Relative surface excess $\Gamma(\varphi,c)$ and surface charge density $\sigma_M(\varphi,c)$ have been computed from the family of electrocapillary curves (Figure 1) as a function of polarization potential φ and solute concentration c (Figures 2 and 3, respectively), following the standard thermodynamical path.[24]

Relative surface excess as a function of surface charge density has been computed by numerical inversion of the function $\sigma_M(\varphi,c)$ to obtain $\varphi(\sigma_M,c)$ and substitution into $\Gamma(\varphi,c)$ to obtain $\Gamma(\varphi(\sigma_M,c),c) = \Gamma(\sigma_M,c)$. This procedure is mathematically equivalent to the use of Parsons' ξ function[25] and more convenient in numerical data handling by digital computers. In fact, experimental data can be arranged as a sequence of triplet $\{\varphi,c,\gamma\}$, each containing values that refer to a single experimental point. Then, each triplet is expanded to a quintuplet $\{\varphi,c,\gamma,\sigma_M,\Gamma\}$, adding the corresponding σ_M and Γ values, computed as described above; the resulting quintuplet sequence can be read selecting two of the five variables, φ, c, γ, σ_M, and Γ, as the independent ones and a third one as function of them.

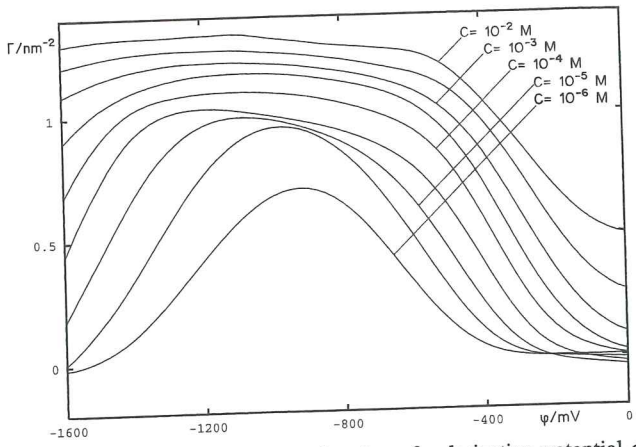

Figure 2. Surface excess Γ as a function of polarization potential φ and solution concentration c.

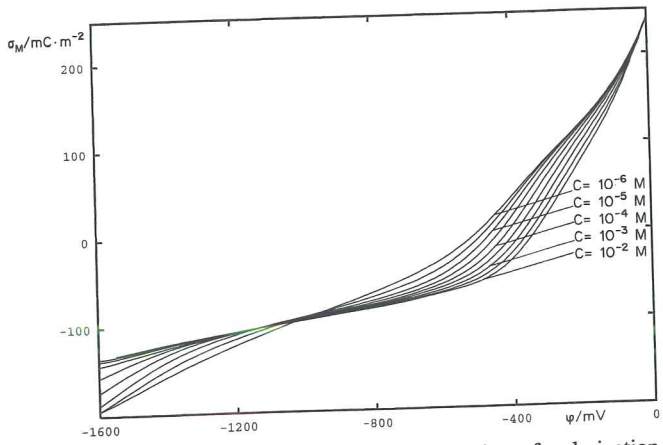

Figure 3. Surface charge density σ_M as a function of polarization potential φ and solution concentration c.

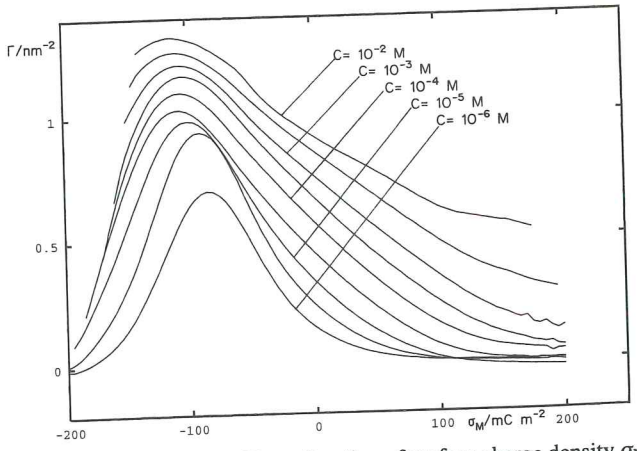

Figure 4. Surface excess Γ as a function of surface charge density σ_M and solution concentration c.

Then, with no further calculation, one can get, e.g., $\Gamma(\varphi,c)$, $\Gamma(\sigma_M,c)$, $\varphi(\sigma_M,c)$, and all other similar useful functions.

Plots of $\Gamma(\sigma_M,c)$ are shown in Figure 4: Bell-shaped curves are obtained, with maxima centered near $\sigma_M = -100$ mC/m^2. A small oscillation in the position of the maximum is clearly seen for the concentration values between $c = 10^{-5}$ and 10^{-4} M that reflects the irregular behavior of the curves in Figure 2 in the same concentration range. To check that this is not an experimental artifact due to lack of equilibrium, an accurate analysis of experimental data is required. Figure 5 shows plots of $\Delta\gamma = \gamma(\varphi,c) - \gamma(\varphi,c=0)$ for several concentrations, as obtained with forward and reverse scan. A clear hysteresis loop can be seen in the two curves at $c = 10^{-6}$ M and, to a minor extent, at $c = 10^{-5.5}$ M. No net effect of this kind can be seen

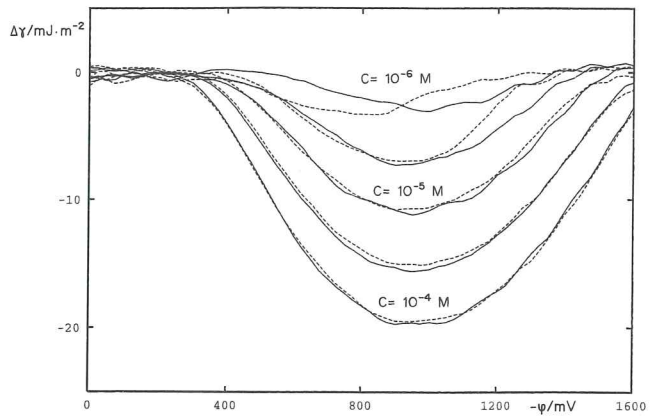

Figure 5. Lowering of the interfacial tension γ as obtained with opposite potential scan: $\Delta\gamma = \gamma(\varphi,c)-\gamma(\varphi,c=0)$. Solid line, direct scan (0 to −1600 mV); dashed line, reverse scan (−1600 to 0 mV).

in the two curves at $c = 10^{-5}$ M, where average difference is 0.01 and 0.42 mJ/m^2 over the potential range $\varphi = -400$ to -900 and -1100 to -1500 mV, respectively. It can be expected that systematic errors due to lack of equilibrium compensate each other to some extent by averaging data taken with opposite scan directions, so that a final worst-case figure sensibly smaller than 0.42 mJ/m^2 should result for the 10^{-5} M curve. On the other hand, the asymmetry in the plots in Figure 2, at the same concentration, would demand an error on γ of the order of 0.8 mJ/m^2 in the −400 to −900 mV potential range, to be explained by lack of equilibrium. Then we exclude the possibility of an experimental artifact; the asymmetry, whose origin remains unexplained, does not affect the following analysis.

Plots in Figures 2 and 4 resemble the usual experimental adsorption behavior of neutral organic compounds, as also predicted by electrostatic adsorption models (see, e.g., refs 26 and 27). This aspect does not contradict the fact that, in the explored concentration range, K222 molecules should be almost entirely in their complexed state with a Na^+ cation inside the cage, as the high value of the K_s constant (7.9×10^3 L/mol)[28] leads to [K222]/[K222$^+$] ≤ 0.2% up to $c = 10^{-2}$ M in a medium containing 0.1 M Na^+.

The ionic contribution in the adsorbed molecules emerges if the adsorption data are parametrized and analyzed according to Frumkin's adsorption isotherm. Among the several isotherm models proposed that differ mainly for the number of adjustable parameters and for the asymptotic conditions at very low or very high surface coverage, Frumkin's isotherm is the most frequently used in the study of organic compound adsorption:

$$\frac{c}{c_0}\frac{\Gamma_M - \Gamma}{\Gamma}\exp(-a\Gamma/\Gamma_M) = \exp(-\Delta G_0/kT)$$

This equation contains three adjustable parameters: Γ_M, the surface excess at maximum coverage, a, the so-called Frumkin's interaction factor, and $c_0 \exp(-\Delta G_0/kT)$, the adsorption factor. The free energy of adsorption, $\Delta G_0/kT$, is measured relative to the choice of the reference concentration c_0 of bulk solution, so that only the whole expression $\beta = c_0 \exp(-\Delta G_0/kT)$ is an independent quantity.

In the case of a polarized interface, the adsorption factor β depends upon the electrical state of the interface. Frequently electrostatic models containing a quadratic dependence of log (β) upon an electrical variable χ, either φ or σ_M, have been used: $\beta = c_0 \exp[(\Delta G_0 + A\chi + B\chi^2)/kT]$.[26] This adds two more parameters to the model, A and B; further "refinements" can be made by adding a dependence of Frumkin's interaction factor

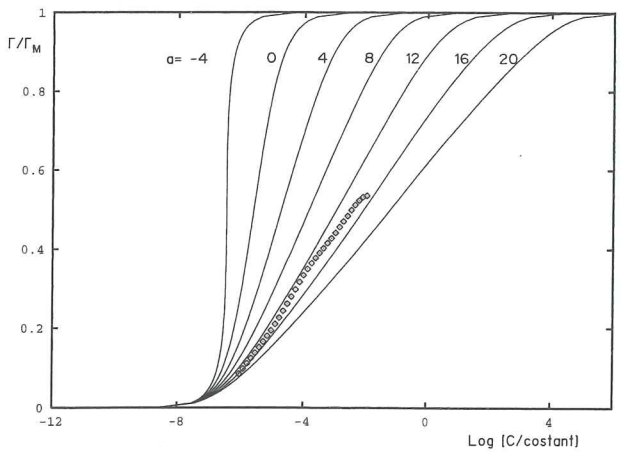

Figure 6. Dependence of coverage Γ/Γ_M as a function of solution concentration, according to Frumkin's isotherm, for various values of the interaction factor a. Diamonds are experimental data for K222 at $\sigma_M = 0$.

a upon Γ and/or the electrical variable, φ or σ_M, thus increasing the number of adjustable parameters well above five. This expansion will not be pursued in this paper.

If adsorption is considered at a fixed electrical state, say $\sigma_M = 0$, Frumkin's isotherm predicts the dependence of Γ vs log (c/β), shown in Figure 6, for several values of the interaction factor a. In this figure we observe that for $a = 0$, i.e., when the actual adsorption state of the surface has no influence on further adsorption or desorption, the transition from clean surface to full coverage, as measured between the concentration $c_{0.1}$ at which $\Gamma/\Gamma_M = 0.1$ and $c_{0.9}$ at which $\Gamma/\Gamma_M = 0.9$, takes place after an increase of concentration c of about 2 decades, independently from the nature of the substance considered and the absolute value of the concentration. Deviations from this universal law are induced by the presence of "interactions" among the adsorbed molecules. These interactions can be either attractive ($a < 0$) or repulsive ($a > 0$). In this context an attractive or repulsive interaction includes, over the direct interactions among the adsorbed molecules, if any, the crossed effect with solvent molecules as well.[27] As is common with aliphatic compounds, an "attractive" interaction factor reflects the decreasing of the number of water−water bonds broken for any further adsorbed molecule as the surface coverage increases. In this condition the transition from clean surface to full coverage can occur with a change in concentration c sensibly smaller than 2 decades, as is the case for 1-octanol.[29] In general, from Frumkin's equation, $\log_{10}(c_{0.9}/c_{0.1}) = 1.91 + 0.35a$.

Data for K222 are shown in Figure 7 for some values of σ_M. It is immediately clear that surface coverage occurs over a range of concentration well wider than 2 decades, extending over more than 4 decades. This can be explained by the presence of a strong repulsive interaction among the adsorbed molecules, which is to be identified with the Coulombian repulsion among the Na^+ cations trapped inside the molecular cage. A quantitative evaluation of the interaction factor requires the knowledge of surface excess Γ_M at full coverage, i.e., when the surface is fully covered by the adsorbed species. This quantity cannot be obtained from experimental data, as in both Figures 2 and 4 there is no evidence of reaching a saturation value in Γ. At the highest concentration attained in these measurements, i.e., $c = 10^{-2}$ M, surface excess amounts to 1.33 molecules/nm^2 at its maximum, corresponding to a surface area of 0.75 nm^2/molecule. The geometrical aspect of K222$^+$, as obtained by computer modeling, when complexed with the cation in the cage, is a spheroid with a minimum area projection $A_e = 0.58$

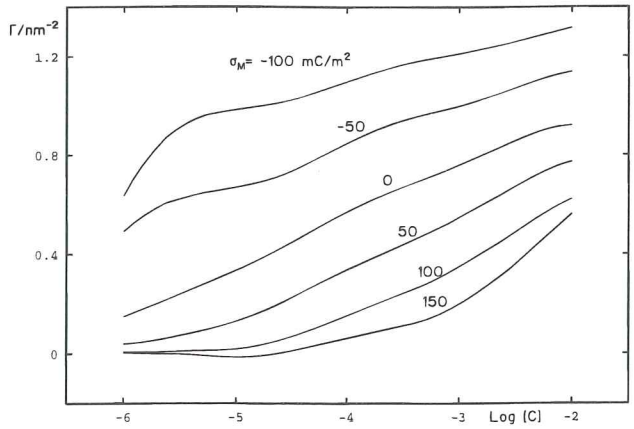

Figure 7. Experimental surface excess Γ as a function of logarithm of concentration, for several values of σ_M.

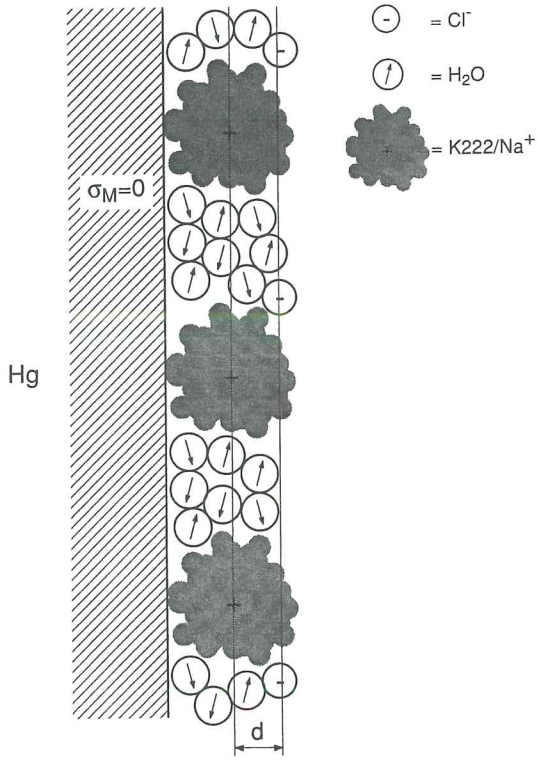

Figure 8. Model of the interfacial region. d is the distance between the distribution of the $K222^+$ and Cl^- ions. ($K222/Na^+ = K222^+$).

nm^2 when the equatorial plane is perpendicular to the adsorbing surface. This gives adsorption saturation at 1.72 molecules/nm^2.

Corresponding values of Γ/Γ_M at $\sigma_M = 0$ are reported in Figure 6 against Frumkin's model plots. Comparing data in Figure 6, a value of $a \simeq 14$ can be hypothesized for the interaction factor in Frumkin's isotherm.

This value points to a repulsive interaction unusually high for a neutral substance, for which a slightly "attractive" term of the order of a few units is common. This repulsion is mainly of electrostatic nature and stems from the cationic charge trapped inside the K222 cage. In fact, as an adsorbed layer of $K222^+$ molecules builds up at $\sigma_M = 0$, a counterion layer rises up to maintain the electroneutrality of the interface (Figure 8). Consequently a double layer builds up in front of the electrode, and even at $\sigma_M = 0$, a potential shift $\Delta\varphi$ results as the surface coverage increases. This effect is shown in Figure 9 for several values of σ_M. It has to be noted that at values of $\sigma_M \neq 0$ this effect cumulates with the potential shift induced by a change in the dielectrical composition of the compact layer in the

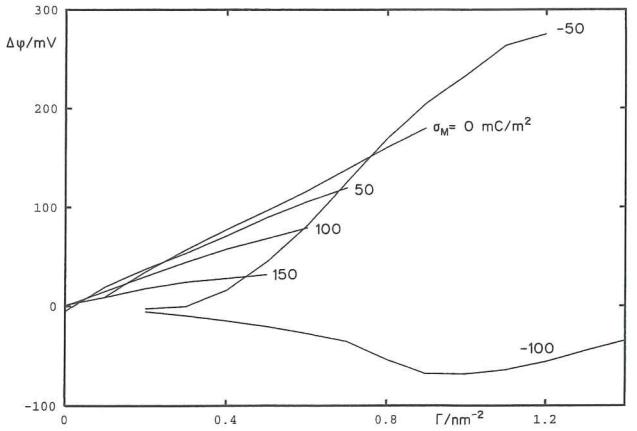

Figure 9. Change in the interfacial polarization potential φ for several values of σ_M, as a function of the surface excess Γ.

presence of the electric field generated by σ_M, making the thorough analysis more complex.

The interaction factor a is, at a first approximation, the (constant) derivative of free energy of adsorption $\Delta G/kT$ with respect to Γ/Γ_M, i.e., $\Delta G/kT = \Delta G_0/kT + a\Gamma/\Gamma_M$. Hence, an electrostatic term $q\Delta\varphi/kT$ has to be added to the free energy of adsorption, if a molecule of K222 that crosses the $\Delta\varphi$ potential region to become adsorbed contains a Na^+ ion inside its cage, with electrical charge q. As the relationship between $\Delta\varphi$ and Γ is linear around $\sigma_M = 0$, as shown in Figure 9, the electrostatic contribute to Frumkin's interaction factor can be written as $a_e = q\Gamma_M/kT\ d\Delta\varphi/d\Gamma \simeq 17$. The agreement between a and a_e is fairly good considering that a contains, in addition to the electrostatic repulsive term a_e, the usual "attractive" term as well, as pointed out above.

Despite the electrostatic nature of the repulsion among the adsorbed K222 molecules, the adsorption driving force remains the usual mechanism of hydrophobic repulsion of the exposed molecular surface, common with aliphatic compounds. In fact, the value of $\Delta G_0/kT$ per unitary cross section surface is 26 nm^{-2}, to be compared with the value of 28 nm^{-2} as obtained from data on aliphatic alcohols and acids reported in ref 30 (Table 4).

The value of $d\Delta\varphi/d\Gamma$ at $\sigma_M = 0$ from data in Figure 9 points to a rather "thin" structure of the $K222^+$–Cl^- sandwich depicted in Figure 8. In fact, considering the system of Figure 8 as a plane symmetry smeared out charge distribution

$$\frac{1}{q}\frac{d\Delta\varphi}{d\Gamma} = \frac{1}{C} = \frac{d}{\epsilon_0\epsilon_R}$$

where C is the capacity per unitary surface of a plane condenser whose thickness d is the average distance between the $K222^+$ and Cl^- plane distributions, ϵ_0 is the dielectric permittivity of vacuum, and ϵ_R is the average relative dielectric constant. Inserting numerical values, $d/\epsilon_R = 0.11$ Å, i.e., the neutralizing Cl^- ions are to be thought as embedded inside the $K222^+$ molecular sheet, the distance between the two plane distributions becomes only a fraction of 1 Å (typical value for ϵ_R is in the range 2–4).

Conclusions

This study shows that relevant information on the adsorption properties of a macrocyclic compound (kryptofix 222) can be obtained from the analysis of electrocapillary curves. In particular we showed that kryptofix 222 strongly adsorbs at the Hg–H_2O interface. This adsorption occurs in the presence of a strong repulsive interaction among the adsorbed K222

molecules that can be identified with Coulomb repulsion due to the Na^+ cations trapped inside the macrocyclic cage. Despite the electrostatic nature of the repulsion among the adsorbed K222 molecules, the adsorption driving force is the common mechanism of hydrophobic repulsion of the exposed molecular surface, as already reported for aliphatic compounds. Moreover the Cl^- counterions are found to be embedded in the $K222^+$ molecular sheet, with the distance between the plane distribution of the $K222^+$ complex and the Cl^- plane being only a fraction of 1 Å. This is also relevant for the interpretation of the results obtained with micellar solution of lithium and sodium dodecyl sulfate in the presence of different macrocyclic compounds, namely, a small macrocyclic cage (CESTO), 18- and 15-crown ethers, and the cryptands K222 and K221. Neutron scattering results[18,19] show that the micellar charge is screened more efficiently by cagelike macrocycles (CESTO and cryptands). This should be related to the driving force which promotes the adsorption at the interface (i.e., the hydrophobic adsorption) and to the presence of an intermolecular repulsive electrostatic interaction that does not allow a fully charge screening upon counterion complexation.

Acknowledgment. This work was funded by grants from INFM, CSGI, and Ministero della Università e della Ricerca Scientifica e Tecnologica (MURST) on "60%" and "40%" funds.

References and Notes

(1) Bajaj, A. V.; Poonia, N. *Coord. Chem. Rev.* **1988**, *87*, 55.
(2) Ringsdorf, H.; Schlarb, B.; Venzmer, J. *Angew. Chem., Int. Ed. Engl.* **1988**, *27*, 113.
(3) Atwood, J. L., Ed. *Inclusion Phenomena and Molecular Recognition*; Plenum: New York, 1990.
(4) Vögtle, F. *Supramolecular Chemistry*; Wiley: New York, 1991.
(5) Gutsche, C. D. *Calixarenes*; The Royal Society of Chemistry: Cambridge, 1989.
(6) Diederich, F. *Cyclophanes*; The Royal Society of Chemistry: Cambridge, 1991.
(7) Gokel, G. W. *Crown Ethers and Cryptands*; The Royal Society of Chemistry: Cambridge, 1991.
(8) Izatt, R. M.; Bradshaw, J. S.; Nielson, S. A.; Lamb, J. D.; Christensen, J. *J. Chem. Rev.* **1985**, *85*, 271.
(9) Izatt, R. M.; Pawlak, K.; Bradshaw, J. S.; Breuening, R. L. *Chem. Rev.* **1991**, *91*, 1721 and references there in.
(10) Monserrat, K.; Graëtzel, M.; Tundo, P. *J. Am. Chem. Soc.* **1980**, *102*, 5527.
(11) Baglioni, P.; Kevan, L. *J. Chem. Soc., Faraday Trans. 1* **1988**, *84*, 467.
(12) Rivara-Minten, E.; Baglioni, P.; Kevan, L. *J. Phys. Chem.* **1988**, *92*, 2613.
(13) Baglioni, P.; Rivara-Minten, E.; Kevan, L. *J. Phys. Chem.* **1988**, *92*, 4726.
(14) Baglioni, P.; Kevan, L. *Prog. Colloid Polym. Sci.* **1988**, *76*, 183.
(15) D'Aprano, A.; Sesta, B. *J. Phys. Chem.* **1987**, *91*, 2415.
(16) Sesta, B.; D'Aprano, A. *J. Phys. Chem.* **1988**, *92*, 2992.
(17) Ozeki, S.; Harada, S.; Kojima, A.; Abe, M.; Ogino, K.; Takahashi, H.; Inokuma, S.; Kuwamura, T. *J. Phys. Chem.* **1990**, *94*, 8213, 8207.
(18) Baglioni, P.; Gambi, C. M. C.; Giordano, R.; Teixeira, J. *Physica B* **1995**, *213/214*, 597−599.
(19) Baglioni, P.; Gambi, C. M. C.; Giordano, R.; Teixeira, J. *Colloid Surf. A*, submitted.
(20) Liu, Y. C.; Baglioni, P.; Teixeira, J.; Chen, S. H. *J. Phys. Chem.* **1994**, *98*, 10208.
(21) Baglioni, P.; Bencini, A.; Dei, L.; Gambi, C. M. C.; Lo Nostro, P.; Chen, S. H.; Liu, Y. C.; Teixeira, J.; Kevan, L. *Colloid Surf. A* **1994**, *88*, 59.
(22) Baglioni, P.; Bencini, A.; Dei, L.; Gambi, C. M. C.; Lo Nostro, P.; Chen, S. H.; Liu, Y. C.; Teixeira, J.; Kevan, L. *J. Phys.: Condens. Matter* **1994**, *6* (Suppl. 23A), 369.
(23) Carlà, M.; Cecchini, R.; Bordi, S. *Rev. Sci. Instrum.* **1991**, *62*, 1088.
(24) Mohilner, D. M. The Electrical Double Layer. In *Electroanalytical Chemistry*; Bard, A. J., Ed.; Dekker: New York, 1969.
(25) Parsons, R. *Can. J. Chem.* **1959**, *37*, 308−314.
(26) Nikitas, P. *J. Electroanal. Chem.* **1994**, *375*, 319−338.
(27) Guidelli, R.; Aloisi, G. Molecular models of organic adsorption from water at charged interfaces. *Electrified interfaces in Physics, Chemistry and Biology*; NATO ASI Series C; Guidelli, R., Ed.; Kluwer Academic Publishers: Dordrecht, 1992; Vol. 355, pp 337−367.
(28) Evans, D. F.; Sen, R.; Warr, G. G. *J. Phys. Chem.* **1986**, *90*, 5500−5502.
(29) Carlà, M.; Aloisi, G.; Moncelli, M. R.; Foresti, M. L. *J. Colloid Interface Sci.* **1989**, *132*, 72.
(30) Bordi, S.; Carlà, M.; Passamonti, P.; Fontanesi, C.; Pelloni, P. *Ber. Bunsen-Ges. Phys. Chem.* **1995**, *99*, 50−58.

JP960031+